Influence of the tensor force on the microscopic heavy-ion interaction potential

Lu Guo (郭璐),[1,2,*] K. Godbey,[3,†] and A. S. Umar[3,‡]

[1]*School of Nuclear Science and Technology, University of Chinese Academy of Sciences, Beijing 100049, China*
[2]*Institute of Theoretical Physics, Chinese Academy of Sciences, Beijing 100190, China*
[3]*Department of Physics and Astronomy, Vanderbilt University, Nashville, Tennessee 37235, USA*

(Received 31 August 2018; published 11 December 2018)

Background: The tensor interaction is known to play an important role in the nuclear structure studies of exotic nuclei. However, most microscopic studies of low-energy nuclear reactions neglect the tensor force, resulting in a lack of knowledge concerning the effect of the tensor force on heavy-ion collisions. An accurate description of the heavy-ion interaction potential is crucial for understanding the microscopic mechanisms of heavy-ion fusion dynamics. Furthermore, the building blocks of the heavy-ion interaction potential in terms of the ingredients of the effective nucleon-nucleon interaction provides the physical underpinnings for connecting the theoretical results with experiment. The tensor force has never been incorporated for calculating the nucleus-nucleus interaction potential.

Purpose: The theoretical study of the influence of the tensor force on heavy-ion interaction potentials is required to further our understanding of the microscopic mechanisms entailed in fusion dynamics.

Method: The full Skyrme tensor force is implemented into the static Hartree-Fock and dynamic density-constrained time-dependent Hartree-Fock (DC-TDHF) theory to calculate both static (frozen density) and dynamic microscopic interaction potentials for reactions involving exotic and stable nuclei.

Results: The static potentials are found to be systematically higher than the dynamical results, which are attributed to the microscopic dynamical effects included in TDHF. We also show that the dynamical potential barriers vary more significantly by the inclusion of tensor force than the static barriers. The influence of isoscalar and isovector tensor terms is also investigated with the T*IJ* set of forces. For light systems, the tensor force is found to have an imperceptible effect on the nucleus-nucleus potential. However, for medium and heavy spin-unsaturated reactions, the potentials may change from a fraction of an MeV to almost 2 MeV by the inclusion of tensor force, indicating a strong impact of the tensor force on subbarrier fusion.

Conclusions: The tensor force could indeed play a large role in the fusion of nuclei, with spin-unsaturated systems seeing a systematic increase in ion-ion barrier height and width. This fusion hindrance is partly due to static, ground-state effects from the inclusion of the tensor force, though additional hindrance appears when studying nuclear dynamics.

DOI: 10.1103/PhysRevC.98.064607

I. INTRODUCTION

With the increasing availability of radioactive ion beams, the study of structure and reactions of exotic nuclei is one of the most fascinating research areas in nuclear physics [1]. The exotic nuclei display distinct features from those seen in typical stable nuclei, which is attributed partly to the unique characteristics of the nucleon-nucleon interaction. The tensor interaction between nucleons is one such characteristic and is well known to be important in nuclear structure properties [2], e.g., the shell evolution of exotic nuclei [3], spin-orbit splitting [4], and Gamow-Teller and charge exchange spin-dipole excitations [5]. However, its role in low-energy nuclear reactions is poorly understood as the tensor force has been neglected in most reaction dynamics calculations. In particular, regarding nuclear dynamics, the tensor force changes not only the spin-orbit splitting but also the intrinsic excitations which may give rise to dynamical effects which are more complicated than those arising from simple shell evolution. The study of the effects of the tensor force on heavy-ion fusion dynamics will lead to a better understanding of the effective nucleon-nucleon interaction and of the correlations present in these many-body systems.

The study of heavy-ion interaction potentials is of fundamental importance for above barrier and subbarrier fusion reactions [6]. In general, two categories of theoretical approaches are used for calculating ion-ion potentials. In the first category, phenomenological models such as the Bass model [7], the proximity potential [8,9], the double-folding potential [10,11], and driven potential from dinuclear system model [12–16] could be mentioned. Although these methods have been successful in explaining particular aspects of reaction data [17,18], the uncertainty of macroscopic parameters and the lack of microscopic origins restrict their predictive power and may obscure the underlying physical processes.

*luguo@ucas.ac.cn
†kyle.s.godbey@vanderbilt.edu
‡umar@compsci.cas.vanderbilt.edu

The second category contains the semi- and fully microscopic approaches to obtain potentials by including the interactions of the constituents [19–23]. One common assumption used in many of the semi-microscopic calculations is that of the frozen density or sudden approximation [24], in which the nuclear densities are unchanged during the computation of the nucleus-nucleus potential as a function of internuclear distance. This approximation may result in an unphysical potential at deep subbarrier energies, where the inner turning point of the interaction potential corresponds to large nuclear overlap. Various remedies were developed to address this issue within the confines of the coupled-channels approach [25,26]. In other microscopic approaches, such as the constrained mean-field methods, although the nuclear densities are allowed for the rearrangement, the potential energy path is obtained by the static adiabatic approximation, thus ignoring the dynamical effects.

In recent years we developed the density-constrained time-dependent Hartree-Fock (DC-TDHF) approach for calculating heavy-ion interaction potentials, which naturally incorporate all of the dynamical effects included in the time-dependent Hartree-Fock (TDHF) description of the collision process [27]. These effects include nucleon transfer, couplings between the collective motion and intrinsic degrees of freedom, neck formation, internal excitations, and deformation effects to all orders. The method is based on the TDHF evolution of the nuclear dynamics coupled with density-constrained (DC) Hartree-Fock (HF) calculations to obtain the ion-ion potential. In contrast to other mean-field-based microscopic methods, the DC-TDHF approach does not need to introduce external constraining operators, which assume that the collective motion is confined to the constrained phase space. That means that the many-body system selects its evolutionary path by itself following the microscopic dynamics. We applied this method for a wide range of reactions [28–37] and found reasonable agreement between the measured fusion cross sections and the DC-TDHF results. To our knowledge, neither the phenomenological nor microscopic methods for calculating ion-ion potential include the tensor force between nucleons, which is an important component of the nuclear force. Our work is an attempt to investigate the effect induced by the tensor force on heavy-ion interaction potentials.

The TDHF approach is a well-defined framework and provides a useful foundation for a fully microscopic many-body theory. Quantum effects are considered, which is essential for the manifestation of shell effects during the collision dynamics. Recently, the effect of the tensor force in heavy-ion collisions has been studied using direct TDHF calculations [38–42]. Furthermore, the TDHF approach provides a deeper understanding of nuclear dynamics, as seen in recent applications to fusion [32–37,43–48], quasifission [49–53], transfer reactions [54–61], fission [62–67], and deep inelastic collisions [39–41,68–74]. For recent reviews see Refs. [75–77].

This article is organized as follows. In Sec. II, we summarize the theoretical formalism of the Skyrme energy functional with the tensor force included and the TDHF and DC-TDHF approaches. Section III presents the systematic analysis of the impact of the tensor force on heavy-ion interaction potentials. A summary is given in Sec. IV.

II. THEORETICAL FRAMEWORK

Despite the wide application of the TDHF approach, various assumptions and approximations that may affect the TDHF results have been employed in the past. This led to an occasional imperfect or even incorrect reproduction of experimental data. To remedy these problems a considerable theoretical and computational effort has been undertaken for increased numerical accuracy and improved effective interactions. For instance, the inclusion of the spin-orbit interaction solved an early conflict between TDHF predictions and experimental observations [78,79] and turned out to play an important role in fusion and dissipation dynamics [68,72]. In recent years it has become feasible to perform TDHF calculations on a three-dimensional Cartesian grid without any symmetry restrictions and with accurate numerical methods. In addition, the quality of the energy density functional (EDF) has been substantially improved. The time-odd terms, in particular, have shown to be nonnegligible in heavy-ion collisions [80]. However, there are still important components of the basic theory that have not yet been fully implemented, such as the tensor force between nucleons. To study the role of tensor force in the heavy-ion interaction potential, we incorporate the full tensor force into the microscopic TDHF and DC-TDHF approaches.

A. Full Skyrme energy functional

Most TDHF calculations employ the Skyrme effective interaction [81], in which the two-body tensor force was proposed in its original form as

$$\begin{aligned} v_T = \frac{t_e}{2}\{&[3(\sigma_1\cdot\mathbf{k}')(\sigma_2\cdot\mathbf{k}')-(\sigma_1\cdot\sigma_2)\mathbf{k}'^2]\delta(\mathbf{r}_1-\mathbf{r}_2)\\ &+\delta(\mathbf{r}_1-\mathbf{r}_2)[3(\sigma_1\cdot\mathbf{k})(\sigma_2\cdot\mathbf{k})-(\sigma_1\cdot\sigma_2)\mathbf{k}^2]\}\\ &+t_o\{3(\sigma_1\cdot\mathbf{k}')\delta(\mathbf{r}_1-\mathbf{r}_2)(\sigma_2\cdot\mathbf{k})\\ &-(\sigma_1\cdot\sigma_2)\mathbf{k}'\delta(\mathbf{r}_1-\mathbf{r}_2)\mathbf{k}\}. \end{aligned} \tag{1}$$

The coupling constants t_e and t_o represent the strengths of triplet-even and triplet-odd tensor interactions, respectively. The operator $\mathbf{k}=\frac{1}{2i}(\nabla_1-\nabla_2)$ acts on the right and $\mathbf{k}'=-\frac{1}{2i}(\nabla_1'-\nabla_2')$ acts on the left.

It is natural to represent the total energy of the system

$$E=\int d^3r\mathscr{H}(\rho,\tau,\mathbf{j},\mathbf{s},\mathbf{T},\mathbf{F},J_{\mu\nu};\mathbf{r}) \tag{2}$$

in terms of the energy functional. The functional is composed by the number density ρ, kinetic density τ, current density $\mathbf{j}$, spin density $\mathbf{s}$, spin-kinetic density $\mathbf{T}$, the tensor-kinetic density $\mathbf{F}$, and spin-current pseudotensor density J [40].

The full version of Skyrme EDF is expressed as

$$\mathscr{H} = \mathscr{H}_0 + \sum_{t=0,1}\Bigg\{A_t^s \mathbf{s}_t^2 + \left(A_t^{\Delta s} + B_t^{\Delta s}\right)\mathbf{s}_t\cdot\Delta\mathbf{s}_t + B_t^{\nabla s}(\nabla\cdot\mathbf{s}_t)^2 + B_t^F\left(\mathbf{s}_t\cdot\mathbf{F}_t - \frac{1}{2}\left(\sum_{\mu=x}^{z} J_{t,\mu\mu}\right)^2 - \frac{1}{2}\sum_{\mu,\nu=x}^{z} J_{t,\mu\nu}J_{t,\nu\mu}\right) + \left(A_t^T + B_t^T\right)\left(\mathbf{s}_t\cdot\mathbf{T}_t - \sum_{\mu,\nu=x}^{z} J_{t,\mu\nu}J_{t,\mu\nu}\right)\Bigg\}, \quad (3)$$

where $\mathscr{H}_0$ is the simplified functional used in the SKY3D TDHF code [82] and most TDHF calculations. The terms containing the coupling constants A arise from the Skyrme central force and those with B from the tensor force. The definitions of both A and B can be found in Refs. [2,83]. All the time-even and time-odd terms in Eq. (3) were implemented numerically in the mean-field Hamiltonians of the HF, TDHF, and DC-TDHF approaches. As pointed out in Refs. [2,40], the terms containing the gradient of spin density may cause spin instability in both nuclear structure and reaction studies, hence the terms of $\mathbf{s}_t\cdot\Delta\mathbf{s}_t$ and $(\nabla\cdot\mathbf{s}_t)^2$ have been turned off in all calculations.

B. TDHF approach

Given a many-body Hamiltonian, the action can be constructed as

$$S = \int_{t_1}^{t_2} dt\,\langle\Phi(\mathbf{r},t)|H - i\hbar\partial_t|\Phi(\mathbf{r},t)\rangle, \quad (4)$$

where Φ is the time-dependent many-body wave function. In the TDHF approach the many-body wave function $\Phi(\mathbf{r},t)$ is approximated as a single time-dependent Slater determinant composed of an antisymmetrized product of the single particle states $\phi_\lambda(\mathbf{r},t)$

$$\Phi(\mathbf{r},t) = \frac{1}{\sqrt{N!}}\det\{\phi_\lambda(\mathbf{r},t)\}, \quad (5)$$

and this form is kept at all times in the dynamical evolution. By taking the variation of the action with respect to the single-particle wave functions, the set of nonlinear coupled TDHF equations in the multidimensional space-time phase space

$$i\hbar\frac{\partial}{\partial_t}\phi_\lambda(\mathbf{r},t) = h\phi_\lambda(\mathbf{r},t) \quad (6)$$

yields the most probable time-dependent mean-field path, where h is the HF single-particle Hamiltonian. The set of nonlinear TDHF equations has been solved on three-dimensional coordinate space without any symmetry restrictions and with modern, accurate numerical methods [80,82].

C. Dynamical potential from DC-TDHF approach

Since TDHF theory describes the collective motion of fusion dynamics in terms of semi-classical trajectories, the subbarrier quantum tunneling of the many-body wave function cannot be included. Consequently, direct TDHF calculations cannot be used to describe subbarrier fusion. At present, all subbarrier fusion calculations assume that there exists an ion-ion potential that depends on the internuclear distance. The microscopic DC-TDHF approach [27] is employed to extract the nucleus-nucleus potential from the TDHF time evolution of the dinuclear system. In this approach, at a certain time during the evolution, the instantaneous TDHF density is used to perform a static HF energy minimization

$$\delta\langle\Psi_{DC}|H - \int d^3r\lambda(\mathbf{r})\rho(\mathbf{r})|\Psi_{DC}\rangle = 0, \quad (7)$$

by constraining the proton and neutron densities to be equal to the instantaneous TDHF densities. Since we are constraining the total density, all moments are simultaneously constrained. DC-TDHF calculations give the adiabatic reference state for a given TDHF state, which is the Slater determinant with the lowest energy for a given density. The minimized energy

$$E_{DC}(\mathbf{R}) = \langle\Psi_{DC}|H|\Psi_{DC}\rangle \quad (8)$$

is the density-constrained energy. Since this density-constrained potential still contains the binding energies of individual nuclei that should be subtracted out, the heavy-ion interaction potential is deduced as

$$V(\mathbf{R}) = E_{DC}(\mathbf{R}) - E_{A1} - E_{A2}, \quad (9)$$

where E_{A1} and E_{A2} are the binding energies of the two individual nuclei. One should note that this procedure does not affect the TDHF time evolution and contains no free parameters or normalization.

D. Bare potential from FHF approach

In the previous subsection, the DC-TDHF technique is introduced to compute the nucleus-nucleus potential in a dynamical microscopic way. All of the dynamical effects included in the TDHF is then directly incorporated in the potential. Here we look for a different approach to produce a bare potential that does not include any dynamical contribution since we aim to disentangle the static and dynamical effects of the tensor force. The bare nucleus-nucleus potential is defined as the interaction potential between the nuclei in their ground states. In addition, to preserve the consistency with microscopic calculations, it is necessary to compute the potential from the same EDF used in HF, TDHF, and DC-TDHF calculations. This is possible using the frozen Hartree-Fock (FHF) technique [84], assuming that the densities of the target and projectile remain constant and equal to their respective ground-state densities. The potential can then be expressed as

$$V_{FD}(\mathbf{R}) = E[\rho_1+\rho_2](\mathbf{R}) - E[\rho_1] - E[\rho_2], \quad (10)$$

where ρ_1 and ρ_2 are HF ground-state densities of the fragments, and $E[\rho_1+\rho_2]$ is the same Skyrme EDF as defined in Eqs. (2) and (3). In the FHF approach, the Pauli principle between pairs of nucleons belonging to different collision partners has been neglected. When the overlap between the density distributions is small, the barrier is almost unaffected by the inclusion of the Pauli principle. However, at larger overlaps of the densities where the Pauli principle is expected to play a more important role, the FHF approximation may not

properly account for the potential, particularly the inner part [48].

III. RESULTS

The concept of using density as a constraint for calculating collective states from TDHF time evolution was first introduced in the mid 1980s [85], and was used for the microscopic description of nuclear molecular resonances [86]. In recent years, the DC-TDHF approach has demonstrated its feasibility and success in explaining subbarrier fusion dynamics for a wide range of reactions. This is rather remarkable given the fact that the only input in DC-TDHF is the Skyrme effective interaction, and there are no adjustable parameters. In the present work, we focus on how the tensor force affects the nucleus-nucleus potential, which is vital for the theoretical analysis of subbarrier fusion dynamics. We thus chose ten representative reactions with proton and neutron numbers of reaction partners corresponding to the magic numbers 8, 20, 28, 50, and 82, in which the spin-saturated shells are 8 and 20.

In the numerical simulation the static HF ground state for the reaction partner was calculated on the symmetry-unrestricted three-dimensional grid. The resulting Slater determinants for each nucleus comprise the larger Slater determinant describing the colliding system during the dynamical evolution. The TDHF time propagation is performed using a Taylor-series expansion up to the sixth order of the unitary boost operator with a time step of 0.2 fm/c. For the dynamical evolution, we use a numerical box of 48 fm along the collision axis and 24 fm in the other two directions and a grid spacing of 1.0 fm. The initial separation between the two nuclei is 20 fm. The choice of these parameters assures good numerical accuracy in the unrestricted TDHF evolution. We simultaneously performed the density constraint calculations utilizing the DC-TDHF method at every 10–20 time steps (corresponding to 2–4 fm/c interval). The convergence property in DC-TDHF calculations is as good if not better than in the traditional constrained HF with a constraint on a single collective degree of freedom.

We employ the Skyrme interaction in the calculations, in which the tensor force has been constructed in two ways. One is to add the force perturbatively to the existing standard interactions, for instance, the existing Skyrme parameter SLy5 [87] plus tensor force, denoted as SLy5t [4]. The comparison between calculations with SLy5 and SLy5t addresses the question on how much of the change is caused by the tensor force itself. Another approach is to readjust the full set of Skyrme parameters self-consistently. This strategy was adopted in Ref. [2] and led to the set of TIJ parametrizations with a wide range of isoscalar and isovector tensor couplings. Due to its fitting strategy, the contributions from the tensor force and the rearrangement of all other terms can be physically entangled.

For light systems, we choose the spin-unsaturated ^{12}C + ^{12}C and spin-saturated ^{16}O + ^{16}O reactions for comparison. As we reported in Ref. [36], the potential barriers are sensitive to the colliding energy. Hence, the same initial energy, close to the Coulomb barrier, is used for the reaction with and without tensor forces. In Fig. 1, we plot the ion-ion potentials obtained from Eq. (9) using the DC-TDHF approach for (a) ^{12}C + ^{12}C at $E_{\rm c.m.} = 8$ MeV and (b) ^{16}O + ^{16}O at $E_{\rm c.m.} = 12$ MeV with SLy5 (open circle) and SLy5t (solid circle) forces. Both nuclei, ^{12}C and ^{16}O, show spherical ground states with tensor (SLy5t) and without tensor (SLy5) forces, which are in agreement with experimental data and other calculations. The correct description of the initial shape of the target and projectile nucleus is important for the dynamical evolution of heavy-ion collisions. We see that for the spin-unsaturated system ^{12}C + ^{12}C, the potential with the tensor force included has an overall higher interaction barrier than without the tensor force, although the difference of the potential barrier peak is small at roughly 0.07 MeV. For the spin-saturated system ^{16}O + ^{16}O, the internuclear potential is close with and without tensor force, having a barrier height of 10.02 MeV and a peak location of 8.66 fm. This indicates that the tensor force has a negligible effect on the near-barrier fusion for the spin-saturated system ^{16}O + ^{16}O, which is consistent with the findings in Ref. [40]. For these light systems the tensor force shows a small effect on the interaction potential.

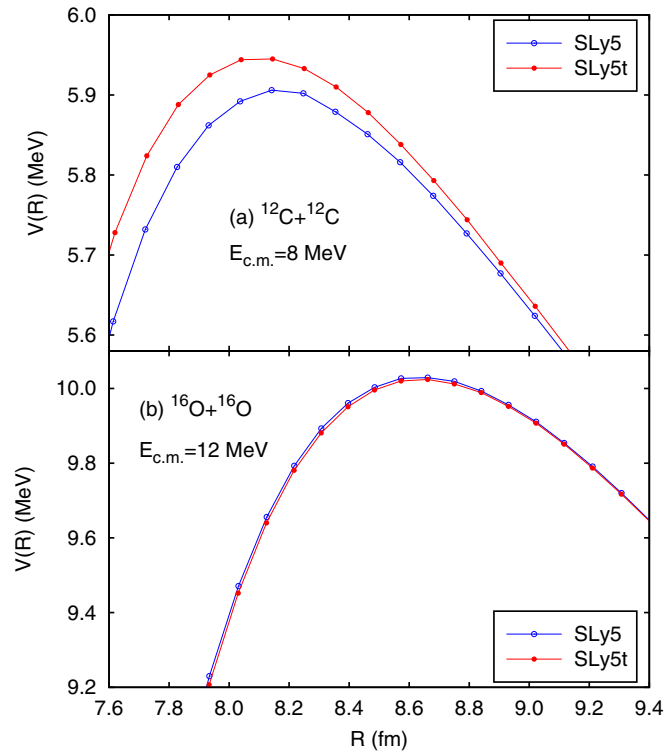

FIG. 1. Internuclear potential obtained from DC-TDHF approach shown for the evolution of the systems (a) ^{12}C + ^{12}C at $E_{\rm c.m.} = 8$ MeV and (b) ^{16}O + ^{16}O at $E_{\rm c.m.} = 12$ MeV with SLy5 (open circle) and SLy5t (solid circle) forces.

For reactions involving two medium mass nuclei, we chose five representative reactions ^{40}Ca + ^{40}Ca, ^{40}Ca + ^{48}Ca, ^{48}Ca + ^{48}Ca, ^{48}Ca + ^{56}Ni, and ^{56}Ni + ^{56}Ni, which vary by the total number of spin-unsaturated magic numbers in target and projectile by 0, 1, 2, 3, and 4. In these collisions, the reaction partners are closed-shell corresponding to 20 (spin-saturated) and 28 (spin-unsaturated) neutron or proton magic numbers. To disentangle the static (e.g., modification of ground-state density) and dynamical (e.g., modification of couplings,

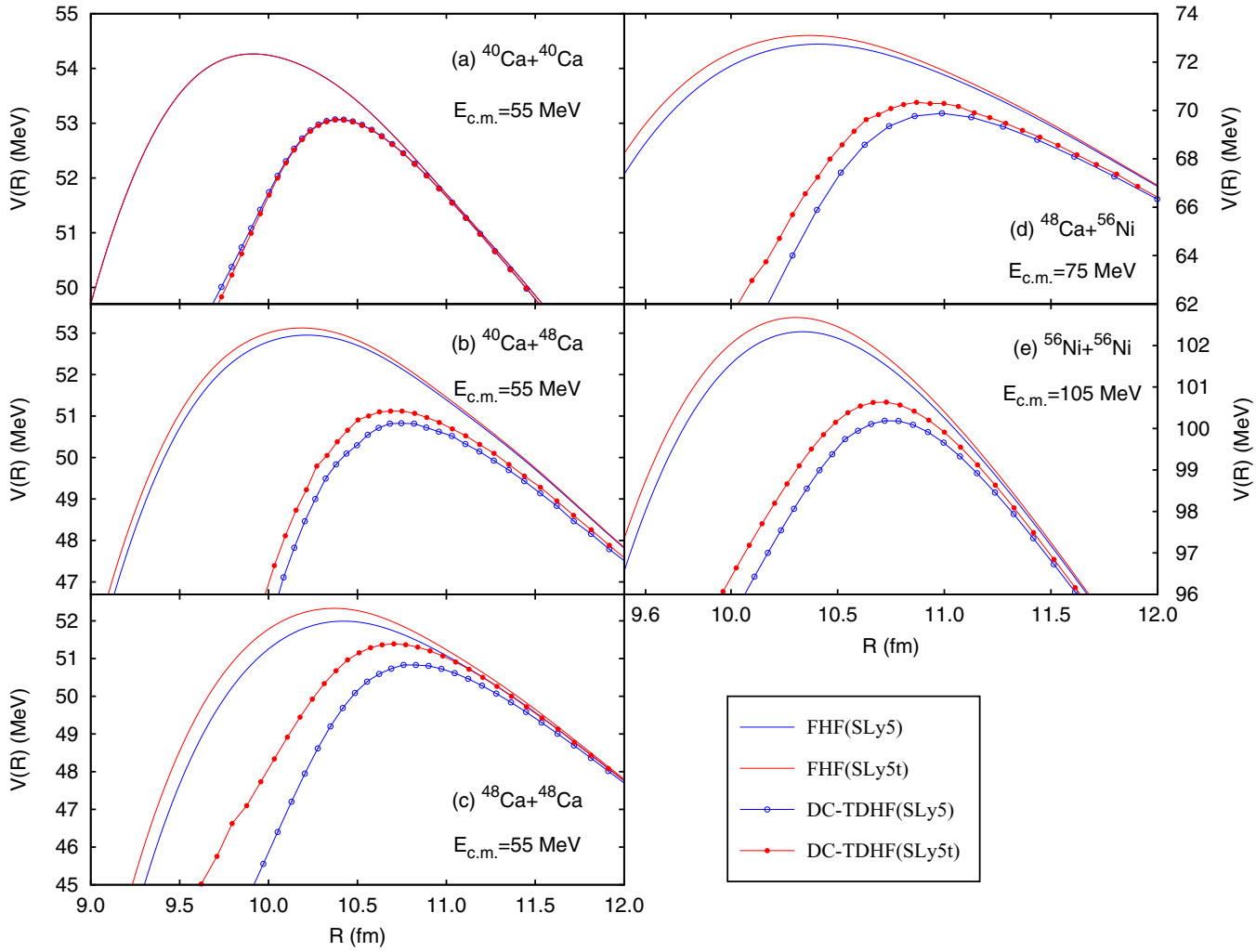

FIG. 2. Internuclear potential obtained from FHF and DC-TDHF approaches for the Ca + Ca, Ca + Ni, and Ni + Ni reactions with tensor (SLy5t) and without tensor (SLy5) forces.

dissipation, and transfer) origins of the tensor force, the nucleus-nucleus potentials obtained both from FHF and DC-TDHF calculations are shown in Fig. 2 for all Ca and Ni reactions. In the initial state of the collision dynamics, the deviation of the static FHF potential from the dynamical DC-TDHF result is the order of smaller than 10 keV. For all the Ca and Ni reactions, we observe that the nucleus-nucleus potentials are considerably different for the static FHF and dynamical DC-TDHF results. The static potentials are systematically higher than the dynamical results, and the barrier peaks are located at smaller relative distance with FHF. In particular, the inner part of the potential, having a strong effect on the subbarrier fusion, presents a more significant difference for FHF and DC-TDHF results. This behavior is well understood and is a consequence of the absence of the Pauli principle and excitations for the frozen density overlaps in FHF potentials [42,48,84], thus the difference between FHF and DC-TDHF is due to dynamical effects. Another interesting observation is that the variation of dynamical barriers due to tensor force is systematically greater than the ones for the static barriers. This indicates that the tensor force influences not only the ground-state single-particle levels, but also the dynamical effects including nucleon transfer, the couplings to low-lying states, and intrinsic excitations. In Ref. [42], how these dynamical effects affect the fusion barriers heights, computed directly from TDHF, were investigated to study the role of tensor force on above-barrier fusion dynamics. We note that in Ref. [42], for the ^{48}Ca + ^{56}Ni system, the tensor force was observed to decrease the barrier height in direct TDHF calculations, which is the opposite of the trend observed here. This difference might arise from the dynamical energy-dependent effects introduced by the tensor force that are not captured by the DC-TDHF potential.

For the spin-saturated reaction ^{40}Ca + ^{40}Ca, the interaction potential remains nearly unchanged by the inclusion of tensor force for both static and dynamical cases, indicating that the tensor force has almost no impact on the dynamical evolution for spin-saturated systems since the contribution of the tensor force is expected to be nearly zero for the ground state of spin-saturated nuclei. For the spin-unsaturated reactions, the barriers with tensor force SLy5t are systematically higher than those without the tensor force SLy5. This indicates a fusion

TABLE I. Isoscalar and isovector spin-current coupling constants in units of MeV fm^5.

Force	C_0^J	C_1^J
T22	0	0
T26	120	120
T44	120	0
T62	120	−120
SLy5	15.65	64.55
SLy5t	−19.35	−70.45

hindrance effect due to the tensor force in this mass region. Empirically, 1 MeV larger in the inner part of the potential barrier can cause one order lower in the fusion cross section at subbarrier energies. From the comparison of dynamical potentials for SLy5 and SLy5t, the potential barrier increases from a fraction up to a few MeV due to tensor force, which may result in changes of the subbarrier fusion cross sections by a few orders of magnitude. For the medium mass systems with proton or neutron magic shells 20 and 28, the tensor force has a significant effect on the nucleus-nucleus potential, particularly in the inner region.

Until now, studies utilized the tensor force SLy5t. To obtain a comprehensive and rigorous understanding of the effects of the tensor force in heavy-ion collisions, we now proceed to a comparison among the results of various forces, for which the coupling constants are listed in Table I. Taking the reaction ^{48}Ca + ^{48}Ca as an example, we show the nucleus-nucleus potential with the six forces SLy5, SLy5t T22, T26, T44, and T62 in Fig. 3. For T22 and T44 the potentials are close to each other, indicating the isoscalar tensor coupling has negligible effect in this reaction. By comparing the results with T26, T44, and T62, the potential increases as the isovector tensor coupling decreases. This clear dependence of isoscalar and isovector tensor coupling may be due to the interplay between tensor terms and the rearrangement of the mean field. The effect of the isoscalar tensor with the proton and neutron

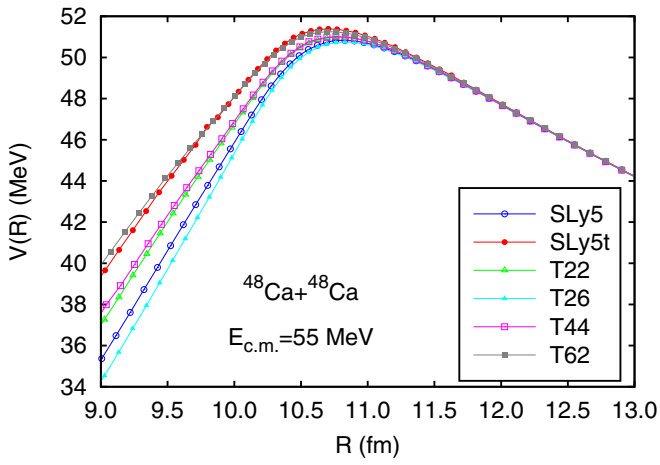

FIG. 3. Internuclear potential obtained from DC-TDHF approach for the reaction ^{48}Ca + ^{48}Ca with SLy5, SLy5t, T22, T26, T44, and T62 forces.

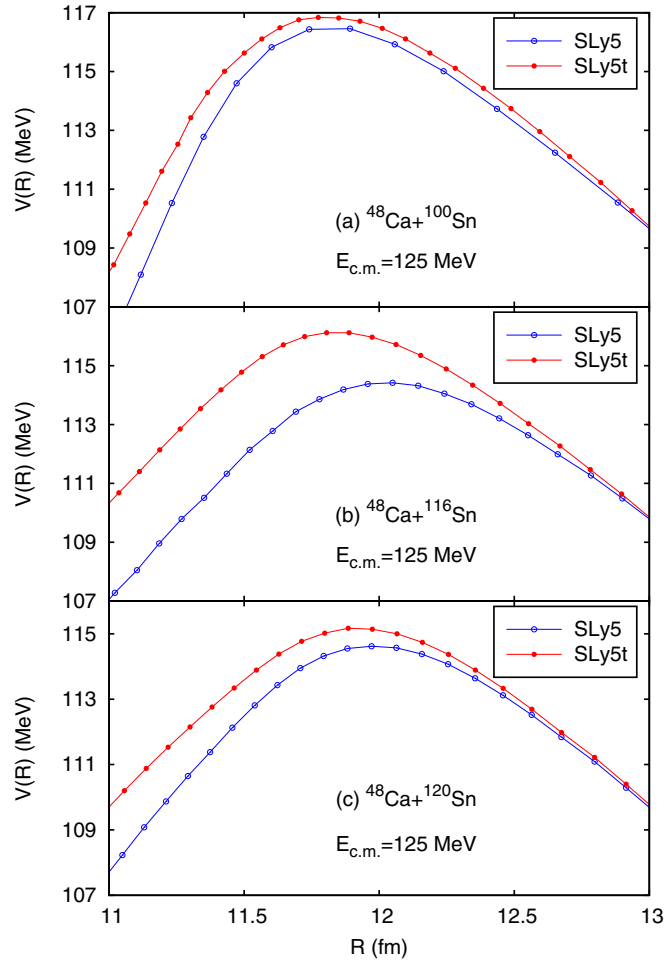

FIG. 4. Internuclear potential obtained from DC-TDHF approach for the Ca+Sn systems with SLy5 (open circle) and SLy5t (solid circle) forces.

single particle spectrum moving in the same way seems to be canceled by the refitting of the parameters. However, the refitting does not incorporate the effect of the isovector tensor in the same way. Detailed discussions on this can be found in Ref. [42]. The T62 (T26) interaction also leads to similar potentials as SLy5t (SLy5), even though they have quite different tensor coupling constants because the rearrangement of the mean field for T62 (T26) produce additional effects that cancel part of the tensor force in SLy5t (SLy5).

To gain a better insight into the tensor force, the dynamical potential is shown in Fig. 4 for various Ca+Sn systems that involve one medium and one heavy reaction partner. For ^{48}Ca, ^{100}Sn, and ^{120}Sn, the ground states are found to be spherical for both SLy5 and SLy5t. However, the ^{116}Sn nucleus exhibits small quadrupole deformation β_2 of 0.077 and 0.026 for SLy5 and SLy5t, respectively, for which the deformation difference arises from the tensor force. Since the outcome of collision dynamics strongly depends on the deformation orientation of colliding partners, the deformed nucleus ^{116}Sn is initially set as the tip orientation in both SLy5 and SLy5t with the symmetry axis of ^{116}Sn parallel to the internuclear axis. We find that, for the Ca + Sn systems, the effects of the tensor

force show similar trends as in the spin-unsaturated Ca + Ca, Ca + Ni, and Ni + Ni systems presented in Fig. 2. The tensor force has the largest effect on the reaction ^{48}Ca + ^{116}Sn as compared to the reactions with ^{48}Ca colliding ^{100}Sn and ^{120}Sn isotopes, which may be due to the strong effect of the tensor force on the energy difference of single-proton states $1h_{11/2}$ and $1g_{9/2}$ along the $Z = 50$ isotopes for ^{116}Sn, as shown in Ref. [4]. Another suspected cause for this large effect arising from the tensor force in the ^{48}Ca + ^{116}Sn reaction is the static deformation effects leading to a vastly different dynamical path for the system.

IV. SUMMARY

We incorporate the full tensor force into the FHF and DC-TDHF approaches to investigate the impact of the tensor force on heavy-ion internuclear potentials for ten representative systems in different mass regimes. As expected we find that static potentials are systematically higher than the dynamical results, however, the variation of dynamical potential barriers induced by tensor force is larger than those of the static case, which are attributed to the microscopic dynamical effects included in TDHF. For light systems, the tensor force is found to have small effects on the nucleus-nucleus potential, with the barrier height and inner part of the barrier changing by a fraction of an MeV. Even this small change may lead to large effects in cross sections when considering deep subbarrier collisions at energy scales common in astrophysical systems. For medium and heavy spin-unsaturated reactions the effect is much more pronounced, with changes from a fraction of an MeV to almost 2 MeV for the barrier height. These differences indicate an important impact on subbarrier fusion dynamics and a substantial fusion hindrance effect arising from the tensor force.

The fully microscopic TDHF theory has shown itself to be rich in nuclear phenomena and continues to stimulate our understanding of nuclear dynamics. The time-dependent mean-field studies seem to show that the dynamic evolution builds up correlations that are not present in the static theory. While modern Skyrme forces provide a much better description of static nuclear properties in comparison to the earlier parametrizations, there is a need to obtain even better parametrizations that incorporate deformation and reaction data into the fit process. The tensor force should be a part of these investigations.

ACKNOWLEDGMENTS

This work is partly supported by NSF of China (Grants No. 11175252 and No. 11575189), NSFC-JSPS International Cooperation Program (Grant No. 11711540016), and Presidential Fund of UCAS, and by the US Department of Energy under Grant No. DE-SC0013847. The computations in present work have been performed on the High-Performance Computing Clusters of SKLTP/ITP-CAS and Tianhe-1A supercomputer located in the Chinese National Supercomputer Center in Tianjin.

[1] A. B. Balantekin, J. Carlson, D. J. Dean, G. M. Fuller, R. J. Furnstahl, M. Hjorth-Jensen, R. V. F. Janssens, B.-A. Li, W. Nazarewicz, F. M. Nunes, W. E. Ormand, S. Reddy, and B. M. Sherrill, Nuclear theory and science of the facility for rare isotope beams, Mod. Phys. Lett. A **29**, 1430010 (2014).

[2] T. Lesinski, M. Bender, K. Bennaceur, T. Duguet, and J. Meyer, Tensor part of the Skyrme energy density functional: Spherical nuclei, Phys. Rev. C **76**, 014312 (2007).

[3] T. Otsuka, T. Matsuo, and D. Abe, Mean Field with Tensor Force and Shell Structure of Exotic Nuclei, Phys. Rev. Lett. **97**, 162501 (2006).

[4] G. Colò, H. Sagawa, S. Fracasso, and P. F. Bortignon, Spin–orbit splitting and the tensor component of the Skyrme interaction, Phys. Lett. B **646**, 227 (2007).

[5] C. L. Bai, H. Q. Zhang, H. Sagawa, X. Z. Zhang, G. Colò, and F. R. Xu, Effect of the Tensor Force on the Charge Exchange Spin–Dipole Excitations of ^{208}Pb, Phys. Rev. Lett. **105**, 072501 (2010).

[6] B. B. Back, H. Esbensen, C. L. Jiang, and K. E. Rehm, Recent developments in heavy-ion fusion reactions, Rev. Mod. Phys. **86**, 317 (2014).

[7] R. Bass, Fusion of heavy nuclei in a classical model, Nucl. Phys. A **231**, 45 (1974).

[8] J. Randrup and J. S. Vaagen, On the proximity treatment of the interaction between deformed nuclei, Phys. Lett. B **77**, 170 (1978).

[9] M. Seiwert, W. Greiner, V. Oberacker, and M. J. Rhoades-Brown, Test of the proximity theorem for deformed nuclei, Phys. Rev. C **29**, 477 (1984).

[10] G. R. Satchler and W. G. Love, Folding model potentials from realistic interactions for heavy-ion scattering, Phys. Rep. **55**, 183 (1979).

[11] M. J. Rhoades-Brown and V. E. Oberacker, Strong Enhancement of Subbarrier Fusion due to Negative Hexadecapole Deformation, Phys. Rev. Lett. **50**, 1435 (1983).

[12] G. G. Adamian, N. V. Antonenko, and W. Scheid, Possibilities of synthesis of new superheavy nuclei in actinide–based fusion reactions, Phys. Rev. C **69**, 044601 (2004).

[13] N. Wang, E.-G. Zhao, W. Scheid, and S.-G. Zhou, Theoretical study of the synthesis of superheavy nuclei with $Z = 119$ and 120 in heavy-ion reactions with trans–uranium targets, Phys. Rev. C **85**, 041601 (2012).

[14] L. Zhu, J. Su, and F.-S. Zhang, Influence of the neutron numbers of projectile and target on the evaporation residue cross sections in hot fusion reactions, Phys. Rev. C **93**, 064610 (2016).

[15] X. J. Bao, Y. Gao, J. Q. Li, and H. F. Zhang, Possibilities for synthesis of new isotopes of superheavy nuclei in cold fusion reactions, Phys. Rev. C **93**, 044615 (2016).

[16] Z.-Q. Feng, Production of neutron-rich isotopes around $N = 126$ in multinucleon transfer reactions, Phys. Rev. C **95**, 024615 (2017).

[17] J. Randrup, Mass transport in nuclear collisions, Nucl. Phys. A **307**, 319 (1978).

[18] G. Fazio, G. Giardina, A. Lamberto, R. Ruggeri, C. Saccá, R. Palamara, A. I. Muminov, A. K. Nasirov, U. T. Yakhshiev, F. Hanappe, T. Materna, and L. Stuttgé, Formation of heavy and superheavy elements by reactions with massive nuclei, Eur. Phys. J. A **19**, 89 (2004).

[19] P. Möller, A. J. Sierk, and A. Iwamoto, Five–Dimensional Fission–Barrier Calculations from ^{70}Se to ^{252}Cf, Phys. Rev. Lett. **92**, 072501 (2004).

[20] L. Guo, F. Sakata, and E.-G. Zhao, Characteristic feature of self–consistent mean–field in level crossing region, Nucl. Phys. A **740**, 59 (2004).

[21] L. Guo, F. Sakata, and E. Zhao, Applicability of self–consistent mean–field theory, Phys. Rev. C **71**, 024315 (2005).

[22] L. Guo, J. A. Maruhn, and P.-G. Reinhard, Triaxiality and shape coexistence in germanium isotopes, Phys. Rev. C **76**, 034317 (2007).

[23] B.-N. Lu, J. Zhao, E.-G. Zhao, and S.-G. Zhou, Multidimensionally–constrained relativistic mean–field models and potential–energy surfaces of actinide nuclei, Phys. Rev. C **89**, 014323 (2014).

[24] K. A. Brueckner, J. R. Buchler, and M. M. Kelly, New Theoretical Approach to Nuclear Heavy-Ion Scattering, Phys. Rev. **173**, 944 (1968).

[25] Ş. Mişicuand H. Esbensen, Hindrance of Heavy-Ion Fusion due to Nuclear Incompressibility, Phys. Rev. Lett. **96**, 112701 (2006).

[26] T. Ichikawa, K. Hagino, and A. Iwamoto, Existence of a one-body barrier revealed in deep subbarrier fusion, Phys. Rev. C **75**, 057603 (2007).

[27] A. S. Umar and V. E. Oberacker, Heavy-ion interaction potential deduced from density-constrained time-dependent Hartree-Fock calculation, Phys. Rev. C **74**, 021601 (2006).

[28] A. S. Umar and V. E. Oberacker, Time dependent Hartree-Fock fusion calculations for spherical, deformed systems, Phys. Rev. C **74**, 024606 (2006).

[29] A. S. Umar and V. E. Oberacker, Dynamical deformation effects in subbarrier fusion of ^{64}Ni + ^{132}Sn, Phys. Rev. C **74**, 061601 (2006).

[30] A. S. Umar and V. E. Oberacker, ^{64}Ni + ^{64}Ni fusion reaction calculated with the density-constrained time-dependent Hartree-Fock formalism, Phys. Rev. C **77**, 064605 (2008).

[31] A. S. Umar, V. E. Oberacker, and J. A. Maruhn, Neutron transfer dynamics and doorway to fusion in time-dependent Hartree-Fock theory, Eur. Phys. J. A **37**, 245 (2008).

[32] A. S. Umar, V. E. Oberacker, J. A. Maruhn, and P.-G. Reinhard, Microscopic calculation of precompound excitation energies for heavy-ion collisions, Phys. Rev. C **80**, 041601 (2009).

[33] V. E. Oberacker, A. S. Umar, J. A. Maruhn, and P.-G. Reinhard, Microscopic study of the ^{132,124}Sn + ^{96}Zr reactions: Dynamic excitation energy, energy-dependent heavy-ion potential, and capture cross section, Phys. Rev. C **82**, 034603 (2010).

[34] R. Keser, A. S. Umar, and V. E. Oberacker, Microscopic study of Ca + Ca fusion, Phys. Rev. C **85**, 044606 (2012).

[35] A. S. Umar, V. E. Oberacker, and C. J. Horowitz, Microscopic sub-barrier fusion calculations for the neutron star crust, Phys. Rev. C **85**, 055801 (2012).

[36] A. S. Umar, C. Simenel, and V. E. Oberacker, Energy dependence of potential barriers and its effect on fusion cross sections, Phys. Rev. C **89**, 034611 (2014).

[37] K. Godbey, A. S. Umar, and C. Simenel, Dependence of fusion on isospin dynamics, Phys. Rev. C **95**, 011601(R) (2017).

[38] S. Fracasso, E. B. Suckling, and P. D. Stevenson, Unrestricted Skyrme-tensor time-dependent Hartree-Fock model and its application to the nuclear response from spherical to triaxial nuclei, Phys. Rev. C **86**, 044303 (2012).

[39] G. Dai, L. Guo, E. Zhao, and S. Zhou, Effect of tensor force on dissipation dynamics in time-dependent Hartree–Fock theory, Sci. China Phys. **57**, 1618 (2014).

[40] P. D. Stevenson, E. B. Suckling, S. Fracasso, M. C. Barton, and A. S. Umar, Skyrme tensor force in heavy ion collisions, Phys. Rev. C **93**, 054617 (2016).

[41] L. Shi and L. Guo, Skyrme Tensor Force in ^{16}O + ^{16}O Fusion Dynamics, Nucl. Phys. Rev. **34**, 41 (2017).

[42] L. Guo, C. Simenel, L. Shi, and C. Yu, The role of tensor force in heavy-ion fusion dynamics, Phys. Lett. B **782**, 401 (2018).

[43] C. Simenel, Ph. Chomaz, and G. de France, Quantum Calculations of Coulomb Reorientation for Sub-Barrier Fusion, Phys. Rev. Lett. **93**, 102701 (2004).

[44] L, Guo and T. Nakatsukasa, Time-dependent Hartree-Fock studies of the dynamical fusion threshold, EPJ Web Conf. **38**, 09003 (2012).

[45] C. Simenel, R. Keser, A. S. Umar, and V. E. Oberacker, Microscopic study of ^{16}O + ^{16}O fusion, Phys. Rev. C **88**, 024617 (2013).

[46] K. Washiyama, Microscopic analysis of fusion hindrance in heavy nuclear systems, Phys. Rev. C **91**, 064607 (2015).

[47] M. Tohyama and A. S. Umar, Two-body dissipation effects on the synthesis of superheavy elements, Phys. Rev. C **93**, 034607 (2016).

[48] C. Simenel, A. S. Umar, K. Godbey, M. Dasgupta, and D. J. Hinde, How the Pauli exclusion principle affects fusion of atomic nuclei, Phys. Rev. C **95**, 031601 (2017).

[49] C. Golabek and C. Simenel, Collision Dynamics of Two ^{238}U Atomic Nuclei, Phys. Rev. Lett. **103**, 042701 (2009).

[50] V. E. Oberacker, A. S. Umar, and C. Simenel, Dissipative dynamics in quasifission, Phys. Rev. C **90**, 054605 (2014).

[51] A. S. Umar, V. E. Oberacker, and C. Simenel, Shape evolution and collective dynamics of quasifission in the time-dependent Hartree-Fock approach, Phys. Rev. C **92**, 024621 (2015).

[52] A. S. Umar, V. E. Oberacker, and C. Simenel, Fusion and quasifission dynamics in the reactions ^{48}Ca + ^{249}Bk and ^{50}Ti + ^{249}Bk using a time-dependent Hartree-Fock approach, Phys. Rev. C **94**, 024605 (2016).

[53] C. Yu and L. Guo, Angular momentum dependence of quasifission dynamics in the reaction ^{48}Ca + ^{244}Pu, Sci. China Phys. **60**, 092011 (2017).

[54] K. Washiyama, S. Ayik, and D. Lacroix, Mass dispersion in transfer reactions with a stochastic mean-field theory, Phys. Rev. C **80**, 031602 (2009).

[55] C. Simenel, Particle Transfer Reactions with the Time-Dependent Hartree-Fock Theory Using a Particle Number Projection Technique, Phys. Rev. Lett. **105**, 192701 (2010).

[56] C. Simenel, Particle-Number Fluctuations and Correlations in Transfer Reactions Obtained Using the Balian-Vénéroni Variational Principle, Phys. Rev. Lett. **106**, 112502 (2011).

[57] G. Scamps and D. Lacroix, Effect of pairing on one- and two-nucleon transfer below the Coulomb barrier: A time-dependent microscopic description, Phys. Rev. C **87**, 014605 (2013).

[58] K. Sekizawa and K. Yabana, Time-dependent Hartree-Fock calculations for multinucleon transfer processes in ^{40,48}Ca + ^{124}Sn, ^{40}Ca + ^{208}Pb, and ^{58}Ni + ^{208}Pb reactions, Phys. Rev. C **88**, 014614 (2013).

[59] N. Wang and L. Guo, New neutron-rich isotope production in ^{154}Sm + ^{160}Gd, Phys. Lett. B **760**, 236 (2016).

[60] K. Sekizawa and K. Yabana, Time-dependent Hartree-Fock calculations for multinucleon transfer and quasifission processes in the ^{64}Ni + ^{238}U reaction, Phys. Rev. C **93**, 054616 (2016).

[61] K. Sekizawa, Enhanced nucleon transfer in tip collisions of ^{238}U + ^{124}Sn, Phys. Rev. C **96**, 041601(R) (2017).
[62] C. Simenel and A. S. Umar, Formation and dynamics of fission fragments, Phys. Rev. C **89**, 031601(R) (2014).
[63] G. Scamps, C. Simenel, and D. Lacroix, Superfluid dynamics of ^{258}Fm fission, Phys. Rev. C **92**, 011602(R) (2015).
[64] P. M. Goddard, P. D. Stevenson, and A. Rios, Fission dynamics within time-dependent Hartree-Fock: Deformation-induced fission, Phys. Rev. C **92**, 054610 (2015).
[65] P. M. Goddard, P. D. Stevenson, and A. Rios, Fission dynamics within time–dependent Hartree–Fock. II. Boost-induced fission, Phys. Rev. C **93**, 014620 (2016).
[66] A. Bulgac, P. Magierski, K. J. Roche, and I. Stetcu, Induced Fission of ^{240}Pu within a Real-Time Microscopic Framework, Phys. Rev. Lett. **116**, 122504 (2016).
[67] Y. Tanimura, D. Lacroix, and S. Ayik, Microscopic Phase–Space Exploration Modeling of ^{258}Fm Spontaneous Fission, Phys. Rev. Lett. **118**, 152501 (2017).
[68] J. A. Maruhn, P.-G. Reinhard, P. D. Stevenson, and M. R. Strayer, Spin-excitation mechanisms in Skyrme-force time-dependent Hartree-Fock calculations, Phys. Rev. C **74**, 027601 (2006).
[69] L. Guo, J. A. Maruhn, and P.-G. Reinhard, Boost-invariant mean field approximation and the nuclear Landau-Zener effect, Phys. Rev. C **76**, 014601 (2007).
[70] L. Guo, J. A. Maruhn, P.-G. Reinhard, and Y. Hashimoto, Conservation properties in the time-dependent Hartree Fock theory, Phys. Rev. C **77**, 041301 (2008).
[71] Y. Iwata and J. A. Maruhn, Enhanced spin-current tensor contribution in collision dynamics, Phys. Rev. C **84**, 014616 (2011).
[72] G.-F. Dai, L. Guo, E.-G. Zhao, and S.-G. Zhou, Dissipation dynamics and spin–orbit force in time–dependent Hartree–Fock theory, Phys. Rev. C **90**, 044609 (2014).
[73] L. Guo, C. Yu, L. Shi, and C. Simenel, Skyrme tensor force in the collision ^{16}O + ^{40}Ca, Eur. Phys. J. Web Conf. **163**, 00021 (2017).
[74] A. S. Umar, C. Simenel, and W. Ye, Transport properties of isospin asymmetric nuclear matter using the time-dependent Hartree–Fock method, Phys. Rev. C **96**, 024625 (2017).
[75] C. Simenel, Nuclear quantum many-body dynamics, Eur. Phys. J. A **48**, 152 (2012).
[76] T. Nakatsukasa, K. Matsuyanagi, M. Matsuo, and K. Yabana, Time-dependent density-functional description of nuclear dynamics, Rev. Mod. Phys. **88**, 045004 (2016).
[77] C. Simenel and A. S. Umar, Heavy-ion collisions and fission dynamics with the time-dependent Hartree-Fock theory and its extensions, Prog. Part. Nucl. Phys. **103**, 19 (2018).
[78] A. S. Umar, M. R. Strayer, and P.-G. Reinhard, Resolution of the Fusion Window Anomaly in Heavy-Ion Collisions, Phys. Rev. Lett. **56**, 2793 (1986).
[79] A. S. Umar, M. R. Strayer, P.-G. Reinhard, K. T. R. Davies, and S.-J. Lee, Spin-orbit force in time-dependent Hartree-Fock calculations of heavy-ion collisions, Phys. Rev. C **40**, 706 (1989).
[80] A. S. Umar and V. E. Oberacker, Three-dimensional unrestricted time-dependent Hartree-Fock fusion calculations using the full Skyrme interaction, Phys. Rev. C **73**, 054607 (2006).
[81] T. H. R. Skyrme, CVII. The nuclear surface, Phil. Mag. **1**, 1043 (1956).
[82] J. A. Maruhn, P.-G. Reinhard, P. D. Stevenson, and A. S. Umar, The TDHF Code Sky3D, Comput. Phys. Commun. **185**, 2195 (2014).
[83] D. Davesne, M. Martini, K. Bennaceur, and J. Meyer, Nuclear response for the Skyrme effective interaction with zero–range tensor terms, Phys. Rev. C **80**, 024314 (2009).
[84] C. Simenel, M. Dasgupta, D. J. Hinde, and E. Williams, Microscopic approach to coupled-channels effects on fusion, Phys. Rev. C **88**, 064604 (2013).
[85] R. Y. Cusson, P.-G. Reinhard, M. R. Strayer, J. A. Maruhn, and W. Greiner, Density as a constraint and the separation of internal excitation energy in TDHF, Z. Phys. A **320**, 475 (1985).
[86] A. S. Umar, M. R. Strayer, R. Y. Cusson, P.-G. Reinhard, and D. A. Bromley, Time-dependent Hartree-Fock calculations of ^{4}He + ^{14}C, ^{12}C + ^{12}C(0^{+}), and ^{4}He + ^{20}Ne molecular formations, Phys. Rev. C **32**, 172 (1985).
[87] E. Chabanat, P. Bonche, P. Haensel, J. Meyer, and R. Schaeffer, A Skyrme parametrization from subnuclear to neutron star densities Part II. Nuclei far from stabilities, Nucl. Phys. A **635**, 231 (1998).